PNAS RESEARCH ARTICLE | BIOPHYSICS AND COMPUTATIONAL BIOLOGY
PLANT BIOLOGY

The carnivorous plant *Genlisea* harnesses active particle dynamics to prey on microfauna

José Martín-Roca[a], C. Miguel Barriuso G.[a], Raúl Martínez Fernández[a], Camila Betterelli Giuliano[b], Rongjing Zhang[c], Chantal Valeriani[a], and Laurence G. Wilson[d,1]

Affiliations are included on p. 6.

Edited by John Brady, California Institute of Technology, Pasadena, CA; received May 13, 2024; accepted November 16, 2024

Carnivory in plants is an unusual trait that has arisen multiple times, independently, throughout evolutionary history. Plants in the genus *Genlisea* are carnivorous and feed on microorganisms that live in soil using modified subterranean leaf structures (rhizophylls). A surprisingly broad array of microfauna has been observed in the plants' digestive chambers, including ciliates, amoebae, and soil mites. Here, we show, through experiments and simulations, that *Genlisea* exploit active matter physics to "rectify" bacterial swimming and establish a local flux of bacteria through the structured environment of the rhizophyll toward the plant's digestion vesicle. In contrast, macromolecular digestion products are free to diffuse away from the digestion vesicle and establish a concentration gradient of carbon sources to draw larger microorganisms further inside the plant. Our experiments and simulations show that this mechanism is likely to be a localized one and that no large-scale efflux of digested matter is present.

active matter | carnivorous plants | statistical physics

Significance

Active suspensions of swimming cells can show complex behavior in confined geometries. Experiments have shown how the swimming direction of bacteria can be rectified by asymmetric obstacles, to bias transport in one direction. This has led to the design of bacterial rotors and ratchets. We have found a naturally occurring bacterial ratchet: carnivorous plants in the genus *Genlisea* grow subterranean structures that exploit nonequilibrium statistical mechanics to supplement their diet in nutrient-poor soils. We show that the passive geometry of the plants' underground structure is sufficient to trap microorganisms, without the need for fluid flow or a chemical lure. Our work shows how an active matter physics principle—bacterial rectification—is harnessed by the natural world.

Carnivorous plants are unusual organisms that survive in nutrient-poor environments by trapping and digesting animal prey, typically insects. Most commonly, this is to supplement their intake of soil macronutrients such as nitrogen and phosphorus (1, 2). Carnivorous plants have adopted a range of prey-capture strategies: pitfall traps (*Sarracenia*, *Nepenthes*, and *Heliamphora*), "flypaper" traps (*Drosera* and *Pinguicula*), and suction traps (*Utricularia*) among others. Carnivory has also given insight into evolutionary biology. Not only is carnivory a rare trait, but there are several evolutionarily distinct lineages that have arrived at the same basic trapping principle—for example, the sticky-leaved flypaper traps of *Byblis* and *Drosophyllum* (3). The genus *Genlisea* is comparatively obscure, though it was included in Darwin's work 'Insectivorous Plants' in 1875 (4). Approximately 30 extant species are distributed across tropical Africa, Central and South America, often in inaccessible and sparsely populated regions.

The parts of *Genlisea* spp. that lie above the surface are superficially unremarkable. The plant is marked by a rosette of small oblong or obovate green leaves, up to a centimeter or so in size. Extending beneath the soil from the main core of the plant are a series of white or translucent tube-like rhizophylls that possess a pronounced bulge (the vesicle) partway along their length, and split into two twisted terminal structures (Fig. 1*A*). From an anatomical point of view, *Genlisea* is rootless (5); these white appendages are underground leaves specially adapted for the capture and digestion of microorganisms. The interior of the rhizophyll is hollow from the vesicle to the spiral-shaped openings at its distal end. The hollow core is filled with rows of detentive hairs that point upward toward the vesicle; these have been posited to act like an eel or lobster trap (6), allowing soil-dwelling organisms such as soil mites to pass inward while making escape difficult. Glands, most densely clustered in the rhizophyll vesicle, secrete digestive enzymes (7–9) which break down prey, and reabsorb nutrients through pores in the cuticle of the digestive glands. The interior milieu of the vesicle has been characterized as mucilaginous (10).

The manner in which *Genlisea* traps its prey remains controversial. Darwin noted that microorganisms entering the branches of the rhizophylls would find their egress prevented by the rows of detentive hairs but stated that it is not clear what would entice the microorganisms to enter in the first place. Furthermore, he noticed that the digestive vesicles of the plant were filled with soil particles and other inorganic debris; this debris is often seen in older rhizophylls and is too large to have arrived there by Brownian motion. Juniper et al. (11) suggest that the plants actively pump fluid into their traps, similar to the closely related bladderworts (*Utricularia* spp.), although at that time there were few studies in living plants, and the flow rates and concomitant energy consumption

Author contributions: C.V. and L.G.W. designed research; J.M.-R., C.M.B.G., R.M.F., C.B.G., R.Z., and L.G.W. performed research; J.M.-R., C.M.B.G., R.Z., C.V., and L.G.W. analyzed data; and J.M.-R., C.M.B.G., R.Z., C.V., and L.G.W. wrote the paper.

The authors declare no competing interest.

This article is a PNAS Direct Submission.

[1]To whom correspondence may be addressed. Email: laurence.wilson@york.ac.uk.

This article contains supporting information online at https://www.pnas.org/lookup/suppl/doi:10.1073/pnas.2409510121/-/DCSupplemental.

Published December 31, 2024.

required to sustain flow seem prohibitive. A recent, detailed structural study (12) has shown that fluid can flow through a rhizophyll much more easily toward the vesicle than away from it. Field studies have consistently found microorganisms, or remnants of them, in the traps of *Genlisea*; these microorganisms including soil mites, protozoa, and bacteria (5, 13). In terms of the benefits to the plant, Barthlott et al. introduced ciliates tagged with ^{35}S and later found the tags had accumulated in the plants' leaves (14). Several authors have speculated upon whether the plant uses an attractant to lure prey into its traps. Darnowski and Fritz (15) tested whether agar that had been placed near *Genlisea* had absorbed any putative 'lure' chemical. The production of lure molecules will incur an energetic cost on the plant, discouraging their creation. In this work, we show that active matter physics principles play a hitherto unrecognized role in the flux of living matter into *Genlisea*.

Over recent decades, Soft Matter Physics and Statistical Physics have given useful insights to unravel features of complex biological phenomena such as cell division, tissue morphogenesis, and population dynamics (16–18). Active matter represents a fundamentally new nonequilibrium branch of soft condensed matter physics, studying out-of-equilibrium systems in which energy is supplied at the level of individual entities and translated into unidirectional motion, for example, "active particles" (19). These dissipate energy while moving (20, 21). Active systems give rise to unexpected collective phenomena not observed in equilibrium systems, from colonies of bacteria to flocks of birds (21–23). Active particles can be synthetic [such as active colloids (24–29)] or living [such as bacteria (30, 31)].

Microorganisms live in environments where viscous forces are orders of magnitude larger than inertial forces (i.e., low Reynolds numbers environments). Here, fluid motion is described by the time-independent Stokes equation. This gives rise to behavior qualitatively different to the macroscopic case, and so analogies drawn between *Genlisea* and human-scale eel traps or lobster pots are only superficial—the physics of swimming is different at the microscale. Bacterial cells (sizes $\sim 10^{-6}$ m) often swim in a series of relatively straight runs (length $\sim 10^{-4}$ to 10^{-5} m) separated by reorientation events. Depending on the species, bacterial reorientations vary from deflections in swimming trajectory (32) through to reversals (33–35) or complete stops (36), during which time Brownian motion reorients cells. One of the most commonly observed swimming phenotypes is the "run-and-tumble" motility observed in soil bacteria such as *Bacillus subtilis* and enteric bacteria such as *Escherichia coli*. When *E. coli* cells are confined in the presence of a microfabricated wall, Galajda and coworkers demonstrated that their motion is rectified by funnel-shaped openings (37), an effect that has been exploited in the design of anti-infection catheters (38). This behavior of swimming bacteria [or other microorganisms (39)] is qualitatively different to that of true Brownian particles (40) and from that of active polar particles (41) in the same confining geometry.

We find that *Genlisea* exploits phenomena observed in the study of active matter in the presence of obstacles to capture prey. We demonstrate how an unusual carnivorous plant has harnessed the rectification of bacterial motion to capture microorganisms, while allowing an attractive chemical gradient of organic molecule to form inside its traps. We first demonstrate that the presence of larger prey microorganisms enhanced transport of environmental debris into the traps, but show no evidence for a chemical "lure" for these organisms. Next, we demonstrate that *Genlisea* can rectify bacterial swimming, and that the hairs rather than a proteinaceous mucilage are likely the dominant contributor to trapping.

Results

Fig. 1*A* shows the gross morphology of an excavated plant, and Fig. 1*B* a scanning electron microscopy cross section of a trap, showing the detentive hairs. To establish a mechanism for large debris to arrive in the vesicle under normal growth conditions (rhizophylls grow downward, so material is transported against gravity), we used fluorescent particles, diameter 15 μm, as probes (Fig. 1*C*). Excised but intact rhizophylls were placed in a sample chamber containing water and probe particles, both with (*Right*-hand side panel) and without (*Left*-hand side panel) ciliate microorganisms (*Paramecium* multimicronucleaton, with cell bodies around 100 μm long and 50 μm in diameter).

To compare rhizophylls of different sizes, we normalized the data by dividing the number of beads counted in a trap (N_{beads}) by the area of the trap "mouth" (A_{mouth}) to give a net flux of beads, as shown in Fig. 1*D*: $\Phi = N_{beads}/A_{mouth}$. The chosen particles were too large to be significantly transported by Brownian motion in the vertical direction. The presence of ciliates (*P.* multimicronucleaton) gives a roughly threefold increase in the number of particles in the vesicles (Fig. 1 *C* and *D*). Therefore, the presence of microorganisms is sufficient to transport inorganic material into the traps. We note that placing rhizophylls in the sample chambers and removing them for particle counting causes a small flow within the sample chamber, which appears to be responsible for some transport, albeit at a lower level: a few particles could be found in the rhizophylls irrespective of the presence of microorganisms.

To investigate the presence or absence of a prey attractant, we built a T-maze choice assay of the type used by van Houten et al. (42) (diagram in Fig. 1*E*), and tested the reaction to soil eluate of ciliates similar to those previously determined to be prey microorganisms (14). Eluate from a pot containing a plant was placed in one test arm of the T-maze, and a control solution in the other. Negative controls were provided by eluate from bare media pots, and by placing eluate in both arms of the maze. A 5 mM solution of NH_4Cl was used as a positive control (42). 5 mL of distilled water containing *P.* multimicronucleaton were placed in the final arm of the T-maze, and the stopcock opened. After 30 min, the stopcock was closed and the ciliates in each arm were counted under a microscope at low magnification and dark field illumination. The effect of the chemical stimulus was measured using the "index of chemokinesis" (χ), reported in Fig. 1*F*:

$$\chi = \frac{N_{test}}{N_{test} + N_{control}}, \qquad [1]$$

where N_{test} and $N_{control}$ are the numbers of cells in the test and control arm of the T-maze, respectively. A value of $\chi = 1$ indicates a chemoattractant strong enough to draw all cells into the test arm of the choice chamber, and a value of $\chi = 0$ corresponds to a perfect repellent (all cells in the control arm). A value of $\chi = 0.5$ corresponds to the null result: the microorganisms are neither attracted nor repelled by the test substance (shown by a continuous line in Fig. 1*F*). The values of χ reported in Fig. 1*F* for two species of *Genlisea* show no clear evidence of a chemical lure for these ciliates.

Previous studies of the carnivory of *Genlisea* have focused on interactions with protozoa, but many smaller microorganisms exist in the soil alongside them. In a nutrient-poor environment,

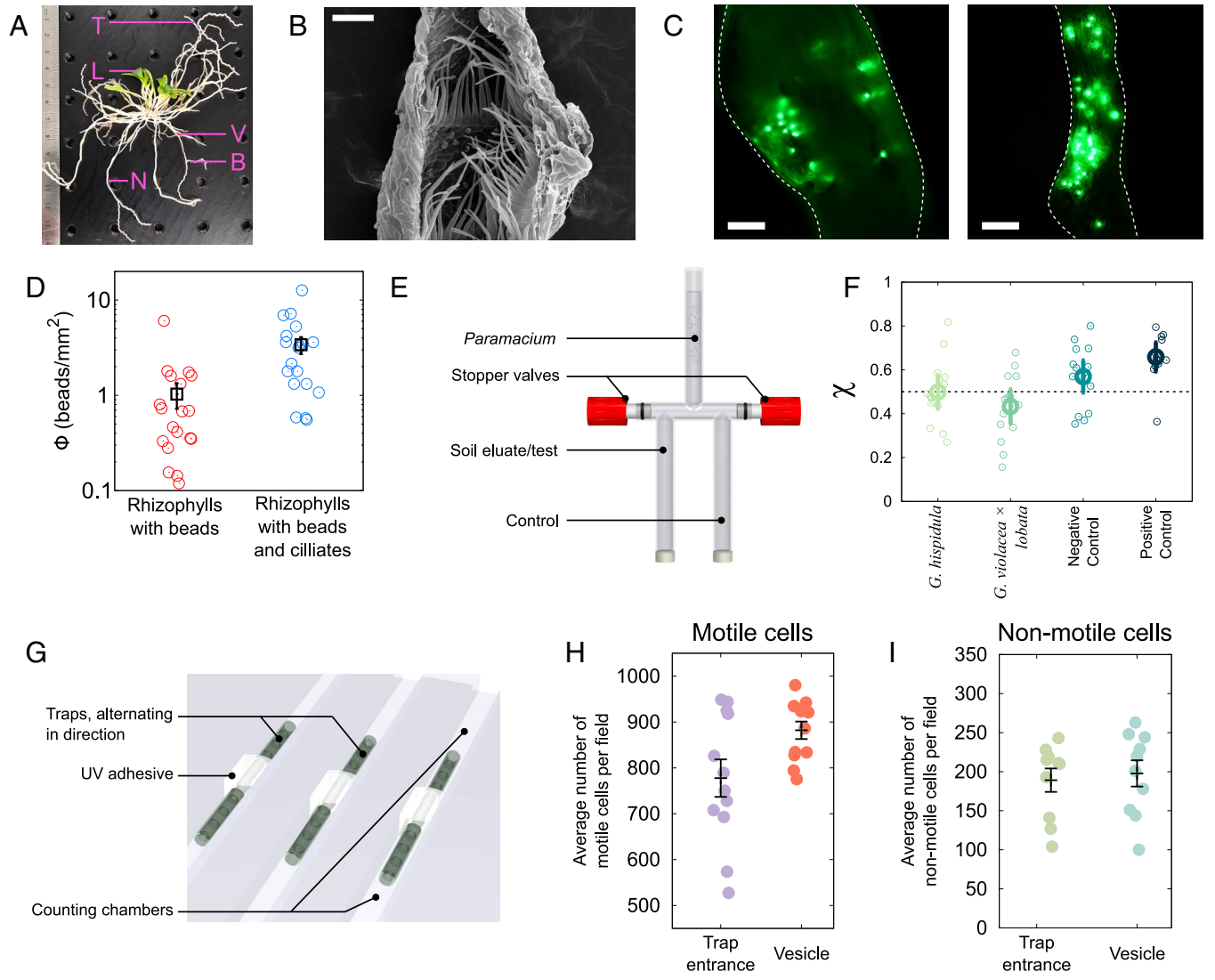

Fig. 1. Experiments showing transport of active and inactive matter. (*A*) Photograph of a *Genlisea hispidula* plant: photosynthetic leaf (*L*), digestive vesicle (*V*), trap neck (*N*), trap bifurcation (*B*), and the characteristic "corkscrew" structure containing the trap openings (*T*). (*B*) A cut-away SEM image showing the interior of one of the traps. The detentive hairs point upward along the rhizophyll's central channel toward the digestive vesicle. (Scale bar, 100 μm.) (*C*) An epifluorescence image of 15 μm tracers inside the vesicle (*Left*) and the trap neck (*Right*) of a *G. hispidula* rhizophyll. (*D*) Concentration of 15 μm fluorescent tracers (normalized by the trap's open area) in the absence (red) or presence (blue) of ciliate prey (mean values in black, errors bars show SEM, Kruskal–Wallis test, $P = 0.0004$). (*E*) Chemotaxis assay chamber presenting different stimuli to planktonic ciliates (see text). (*F*) Chemokinesis coefficients. Each point corresponds to an experiment involving an initial loading of around 150 ciliates. Large data points indicate the mean, and the error bars show 95% CI. The horizontal black line represents the null hypothesis. (*G*) A "cartoon" of the bacterial rectification setup, with a section of rhizophyll trap neck connecting two chambers. (*H*) Number of motile cells at each end of the trap neck section after two hours (black data points represent mean and SEM, two-tailed paired *t* test, $P = 0.030$). The average velocity of the motile cells was ~ 16 μm/s (*SI Appendix*, Fig. S2). (*I*) Number of nonmotile cells at each end of the trap neck section after 2 h (black data points represent mean and SEM, two-tailed paired *t*-test, $P = 0.697$).

a broader prey spectrum increases the chances that nutritional requirements will be met. It has been estimated that there are between 10^4 and 10^5 protozoa per gram of soil (43), compared to around 10^8 bacteria in the same mass (44). The biomasses of these categories are therefore likely to be similar. Rhizosphere microbiomes are complex (45), but the swimming phenotype of common model soil-dwelling and root-associated bacterial species such as *B. subtilis* is a canonical run-and-tumble quantitatively similar to *E. coli* (46). The size and arrangement of detentive hairs within the rhizophylls are reminiscent of microfabricated devices used in previous studies of active matter systems (37, 47, 48). Inspired by such results, we prepared chambers divided into two, with the halves bridged by excised rhizophylls (shown in cartoon form in Fig. 1*G*). The rhizophylls were aligned in opposite directions in alternating channels, and both halves of the chambers filled with an initially uniform concentration of *E. coli*. After two hours, bacteria in a 2 mm^2 field of view at either end of each rhizophyll were counted. As shown in Fig. 1*H*, we observed an enrichment of 10 to 15% in the number of cells present at the end of the rhizophyll previously connected to the vesicle (as compared to the trap entrance). No such enrichment is observed in the case of nonmotile cells (Fig.1*I*).

We use this information to guide numerical simulations that untangle the relative importance of different aspects of the trap structure. We simulated suspensions of run-and-tumble particles (disk-like, with diameter σ and propulsion speed of v) confined in a channel. Fig. 2*A* represents typical trajectories of active particles in the funneled channel, mimicking the plant's hair and whose geometry has been tailored borrowing parameters from

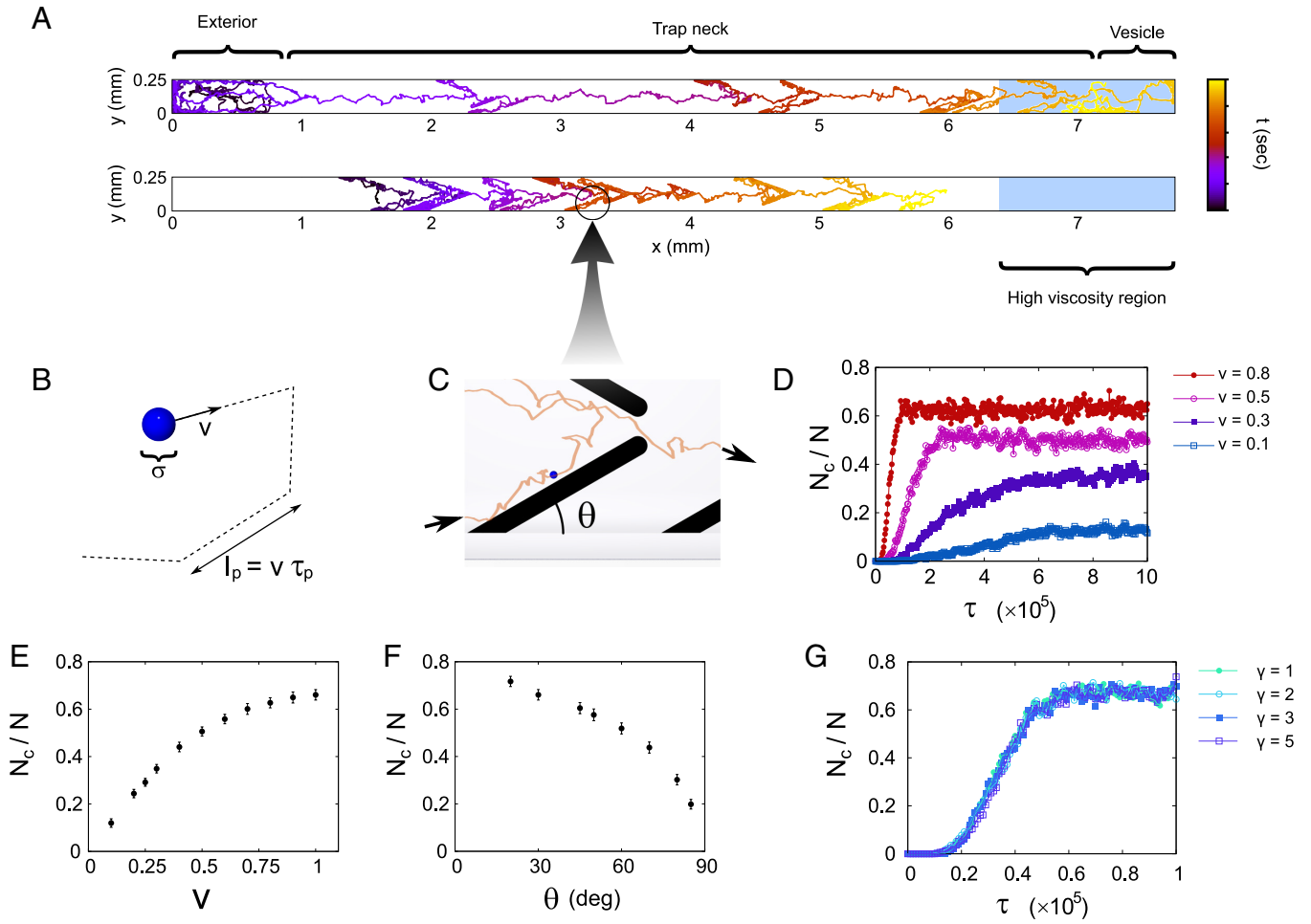

Fig. 2. Geometrical contributions to carnivorous trapping. (*A*) Trajectories of simulated bacteria within the rhizophyll of *Genlisea*, with dimensions taken from experiments. The detentive trap hairs have been omitted for clarity. The structures have three regions including an "exterior" (no hairs), neck (with hairs), and vesicle (no hairs, but variable friction). (*B*) A cartoon showing characteristic swimming mode and parameters for the bacterium: size (σ), speed (v) persistence time (τ_p), and persistence length ($l_p = v\tau_p$). (*C*) Subsection of a particle trajectory from panel *A* showing a simulated bacterium interacting with a hair. The hair lies at an angle θ to the rhizophyll wall; black arrows show the direction of the bacterium's travel. (*D*) The fraction of trapped cells N_c/N (trapping efficiency, where N_c is the number of cells captured in the vesicle and N is the total number of cells) for a fixed trap geometry ($\theta = 30°$) and variable swimming speed. Both trapping rate (initial gradient) and saturation occupancy (plateau level at late times) increase with v; the time is indicated in nondimensionalized simulation units. (*E*) The saturation level of N_c/N as a function of swimming speed. The escape probability decreased with l_p. (*F*) Dependence of trapping efficiency on the hair angle θ, for hairs with a fixed projection on the y-axis (see text) and swimming speed $v_p = 1$. Smaller angles lead to more efficient trapping, but require longer hairs to be grown if the gap between hairs at the center of the channel remains constant. (*G*) The effect of decreased mobility within the vesicle on trapping efficiency. There is no apparent evidence that increasing the friction coefficient in the vesicle increases trapping; the hairs are therefore the dominant contribution to prey trapping.

experiments: the individual tracks are color-coded to indicate time. Detentive hairs within the traps have been omitted for clarity, but their influence can be seen in the chevron-shaped deviations in the trajectories, which lead to the trap vesicle on the right. In our study the funnel-shaped obstacles along the channel are straight; allowing them to be curved seems to have a minimal effect on the dynamics of the system (*SI Appendix*). The particles' motion is characterized by a persistence length $l_p = v\tau_p$, where τ_p is the persistence time or the time between reorientations (Fig. 2*B*). Two-dimensional numerical simulations were carried out (see *SI Appendix* for details). All particles start in the exterior region as an initial configuration, and their positions evolve until they reach a steady state. Interactions with the detentive hairs are shown in Fig. 2*C*, where θ is the angle that the hairs make with the rhizophyll wall. Two-dimensional simulations make the trapping process much simpler to visualize and analyze, as well as lowering their computational cost. The true three-dimensional equivalent of our simulations would be a series of solid funnels—this is a reasonable approximation of the internal structure of a *Genlisea* rhizophyll, in which hairs broaden toward their base, forming an almost continuous barrier at the rhizophyll wall.

To quantify the trapping efficacy, we examine the rate of accumulation in the vesicle, as well as the final (steady state) fraction of cells located there. Fig. 2*D* shows the time dependence of cell accumulation, for cells with different swimming speeds ($v = 0.1$ to 0.8, as indicated in the legend). Intuitively, cells that swim faster accumulate more quickly in the vesicle. The "toy model" invoked is clearly sufficient to allow trapping of bacteria in the vesicle: the vesicle comprises 10% of the length of the rhizophyll, but accommodates at least 15% of the cells, even in the case of the weakest trapping, rising to over 60% of cells for the strongest trapping. If the cells' tumble rate is held constant but the speed is varied, this will give rise to a longer persistence length l_p. This results in a more efficient rectification of the swimming behavior, and therefore a greater fraction of cells accumulating within the vesicle.

Nevertheless, the stochastic swimming process does offer cells a chance of escape. Fig. 2*E* shows the steady-state accumulation of cells in the vesicle, as a function of swimming speed. The

accumulation saturates with around 65% of the cells in the vesicle, presumably limited by cells stochastically escaping the trap. Comparing our microscopy studies to those of other authors, we find that the detentive hairs within the rhizophyll vary in length somewhat between species (5), and within individual rhizophylls (12). We have chosen an intermediate, constant hair length in our simulations for the sake of simplicity. A recent study on the energetics of rectification suggests that in two dimensions, and with obstacles closer in size to bacteria, an angle between barriers of 120 degrees (corresponding to a hair angle of 60 degrees in our system, chosen based on observations from SEM measurements, see *SI Appendix*, Table S1) is approximately optimal (49). It would be intriguing to see whether these findings extend to the larger, three-dimensional case of *Genlisea*.

Finally, we investigated the effect of the mucilaginous plug that has been observed in the vesicle of species of *Genlisea*. It is difficult to determine definitively whether the mucilage is a product of the plant or a consequence of the digestion of microbes. Nevertheless, its rheology may have consequences for the trapping behavior of the plant. In a situation where the viscosity is variable, we anticipate that purely Brownian diffusing particles will have a distribution $\rho(r)$ that is uniform because $\rho(r) \sim \exp\left[-\frac{U(r)}{k_B T}\right]$ at equilibrium, and the potential U(r) is constant. Conversely, swimming particles accumulate in regions of lower mobility. We therefore perform simulations in which the stomach region has increased friction γ, Fig. 2*G*. These show that the effect of lower particle mobility has only a marginal trapping effect and that the accumulation in the vesicle is governed by the geometry of hairs in the rhizophyll channel.

Conclusion

We have shown that plants in this fascinating genus constitute a naturally occurring active matter rectifier, allowing them to increase their supply of nutrients in an otherwise nutrient-poor environment by selectively trapping bacterial prey. Darwin's "eel trap" description (4) was based on observations of microfauna that became stuck in *Genlisea* rhizophylls, unable to escape. We show that the same structures that trapped these arthropods are sufficient to guide bacteria—orders of magnitude smaller—to the plant's digestive vesicles. Moreover, we explain the presence of large soil particles in the vesicle without recourse to an active mechanism such as fluid flows [for which there is little evidence in this genus (50)], but find no evidence for a chemical lure, at least one suitable for attracting a common genus of ciliate. Establishing the full role of bacterial species inside the rhizophylls will be a fascinating area for future work: some species may be prey, while others could form part of a food web within the traps (9, 13), breaking down constituents of other microorganisms into forms that the plant can absorb. Although this plant is considered a "true" carnivore due to its production of digestive enzymes (51), carnivory is a spectrum, with genera such as *Roridula* using symbiosis with insect commensals to facilitate prey digestion (52). Our study raises the intriguing possibility of non- or quasi-carnivorous subterranean structures in a potentially wide range of other plants that use quirks of their morphology to sequester microorganisms that then die near to the plant, releasing nutrients—a web of subtle carnivory beneath our feet.

Materials and Methods

Plant Growth. Experiments were conducted on *G. hispidula*, with additional measurements on *Genlisea lobata* × *violacea* in the case of the chemoattractant tests. The plants were grown in 5 cm pots filled with a 1:1:1 peat-sand-perlite soil medium. Each pot was placed into an individual plastic cup within the terrarium to prevent the water outflow from each pot mixing together (necessary for the chemotaxis experiments). The plants were watered with distilled water and placed on a 16-h photoperiod under "cool white" compact fluorescent lamps (color temperature 6,500 K). During cultivation, a USB data logger was used to record the average temperature and relative humidity in the terrarium: around 24 °C and 45% humidity during the day and 19.5 °C at night with 65% humidity. The microscopy experiments were conducted at the ambient temperature of the lab (away from the fluorescent lighting) of 21±1°C. The SEM image in Fig. 1*B* is from *G. hispidula*, prepared according to the protocols provided in previous studies (5, 10, 11).

Transport of Debris Into Vesicles. As previously stated, inorganic debris is found inside the digestive vesicle of *Genlisea* spp., and this debris must be actively moved into the traps against gravity. The most likely agent seems to be the prey animals that live in the surrounding environment. To test the hypothesis that prey animals push inorganic material into the traps, several plantlets of *G. hispidula* were excavated and washed thoroughly with distilled water. Around six rhizophylls were excised from the plants and cut above the digestive vesicle so that the hollow rhizophyll channel was maintained. The plants and excised traps were placed in separate petri dishes, which were divided into two groups, test and control. Petri dishes in the test group contained a suspension of fluorescent beads (diameter 15 μm, "dragon green," Bangs Labs Inc.) mixed with a culture of the ciliate *Paramecium* multimicronucleaton (Carolina Biological Supply Co.); the control group of petri dishes contained only a suspension of beads (at the same concentration as the test dishes). The particles that we use are too large to be significantly transported by Brownian motion in the vertical direction; we would expect their concentration do decrease exponentially against gravity, with the characteristic length scale given by Perrin (53), $l_c = k_B T/m^* g$, where $k_B T$ is the thermal energy, m^* is a particle's buoyant mass and g is acceleration due to gravity. For particles the size of ours, $l_c \approx 5$ μm, so we expect the fluorescent tracers to lie more or less in a layer on the bottom surface of the petri dish, though they are free to diffuse in the horizontal plane.

After 7 d, plants and traps were washed extensively with distilled water and analyzed under a fluorescence microscope. The number of beads found inside each trap was recorded by eye, refocusing the microscope as appropriate to count particles. Bleaching was not apparent over several minutes of observations with these large particles. As can be seen in Fig. 1*A*, the rhizophylls from a single plant are often of different sizes, with different trap thicknesses and lengths. To make a valid comparison between rhizophylls, we normalize the number of beads each trap ingested by its effective opening ("mouth") size, giving a total flux of Φ beads/mm^2. The trap shapes are rather complicated, so we modeled each trap arm as a cylinder with an opening fraction per unit surface area, and the mouth region at the trap bifurcation as an open rectangle. The dimensions of the trap were determined by digital photographs.

Presence of a Chemoattractant. To test for the presence or absence of a soluble chemoattractant produced by the plant, we initially attempted some holographic particle tracking (33, 54) to see whether the swimming patterns of *P.* multimicronucleaton were modified when swimming close to the rhizophyll. These results were inconclusive so instead we performed a T-maze choice assay of the type used by van Houten et al. (42) (as in Fig. 1*E*). Five pots containing *G. hispidula* plants, five containing *G. lobata* × *violacea*, and five pots containing bare potting media without *Genlisea* were kept in the conditions described above. Each pot was placed in an individual plastic cup so that the water outflow from the pots could not mix together. After 3 mo, each pot was washed through with around 50 mL of distilled water, and the eluate that accumulated in the plastic cups was collected. The eluate from a pot containing a plant was placed in one test arm of the T-maze, and a control solution in the other. Negative controls were provided by the eluate from bare media pots, and by comparing plant solutions to themselves. A 5 mM solution of NH_4Cl was used as a positive control (42). 5 mL of distilled water containing *P.* multimicronucleaton was placed in the final arm of the T-maze, and the stopcock opened. After 30 min, the stopcock was closed and the ciliates in each arm were counted under a microscope at low

magnification and dark field illumination. The effect of the chemical stimulus was measured using the index of chemokinesis χ (Eq. **1**).

Bacterial Rectification. To demonstrate that the rhizophyll "neck" is capable of rectifying bacterial swimmers, an assay was developed as pictured in Fig. 1*G*. Channels measuring 50 mm × 4 mm × 3 mm were constructed from UV-curing glue and glass slides. 2 cm sections of trap necks cut from *G. hispidula* were carefully washed in DI water and placed in the channels. These were sealed in place using UV curing glue to give an external barrier between the ends of the neck sections. The chambers were then filled with a suspension of *E. coli* bacteria in tryptone broth as described previously (55). The suspension initially occupied both halves of the chamber, with bacteria at a uniform concentration. After a period of 2 h, the numbers of swimming cells immediately adjacent to the neck openings was measured. The experiment was then repeated with cultures of cells that had been heated to 65 °C to deactivate them. For the analysis, normality was assessed using the Shapiro–Wilk test.

Simulation Details. To explore the hypothesis of living particles being trapped inside the rhizophylls, we numerically study the relationship between the motion of prey organisms and the hair geometry. Based on the experimental observation of ref. 37, our model consists of a two-dimensional system of N run-and-tumble particles. The active particles of diameter σ are kept in a two-dimensional closed geometry which consists of a channel with hairs at regular distances, of identical shape and orientation. Channel hairs are composed of nonmotile circles, while the channel's walls are directly simulated as straight boundaries. This geometry (shown in cartoon form in Fig. 2*A*), is a simplified representation of a rhizophyll. Particles move due to self-propulsion in a straight line at speed v during a period of time τ_p, after which they randomly change their direction of motion, but not their speed. Interactions between particles and with the walls of the channel are solved via a Molecular Dynamics algorithm computing the interacting forces between particles using a WCA potential (see *SI Appendix* for more details). We consider a channel of width $Ly = 25\sigma_0$ and length $L_x = 775\sigma_0$, containing particles of diameter σ_0 at a number density $\rho = 0.1\sigma_0^{-2}$. The distance between consecutive hairs along the walls is $d = 25\sigma_0$. The opening between opposing hairs in the channel is $3\sigma_0$. In Fig. 2*E*, the values used for the simulations are $\theta = 60°$ (tilt angle of the hairs with respect to the longitudinal axis of the channel), $v = 1.0\sigma_0/\tau_0$, $\tau_r = 1.0\tau_0$, $k_BT = 1.0\epsilon_0$, $\gamma_0 = 1.0\, m_0/\tau_0$, $m = m_0$ where τ_0, ϵ_0, m_0, and σ_0 are Lennard–Jones units for time, energy, mass, and distance, related as $\epsilon_0 = m_0\sigma_0^2/\tau_0^2$. The channel is divided into 3 sectors: mouth ($0 < x < 75\sigma_0$), root ($75\sigma_0 < x < 700\sigma_0$), and stomach ($700\sigma_0 < x < 775\sigma_0$) in every simulation. The right-most section is considered as the stomach and the particles lying there are considered trapped, for counting purposes.

Data, Materials, and Software Availability. All study data are included in the article and/or supporting information.

ACKNOWLEDGMENTS. We thank L. Turner, S. J. Davis, and A. Fitter for helpful discussions and J. Chervinsky for assistance in preparing the SEM figure. This work was supported by the Rowland Institute at Harvard (L.G.W. and R.Z.), Coordenação de Aperfeiçoamento de Pessoal de Nível Superior 7340/11-7 This author should be C.B.G., MINECO IHRC22/00002, and PID2022-140407NB-C21 (C.V.).

Author affiliations: [a]Departamento de Estructura de la Materia, Fisica Termica y Electronica, Facultad de Ciencias Fisicas, Universidad Complutense de Madrid, Madrid 28040, Spain; [b]Elvesys—Microfluidics Innovation Centre, Paris 75011, France; [c]Department of Physics, University of Science and Technology of China, Hefei 230026, Anhui, China; and [d]School of Physics, Engineering & Technology, University of York, Heslington, York YO10 5DD, United Kingdom

1. A. Ellison, Nutrient limitation and stoichiometry of carnivorous plants. *Plant Biol.* **8**, 740–747 (2006).
2. V. Albert, R. Jobson, T. Michael, D. Taylor, The carnivorous bladderwort (Utricularia, Lentibulariaceae): A system inflates. *J. Exp. Bot.* **61**, 5–9 (2010).
3. V. Albert, S. Williams, M. Chase, Carnivorous plants: Phylogeny and structural evolution. *Science* **257**, 1491–1495 (1992).
4. C. Darwin, *Insectivorous Plants* (John Murray, London, UK, 1875).
5. A. Fleischmann, *Monograph of the Genus Genlisea* (Redfern Natural History Productions Ltd., 2012).
6. B. Plachno, M. Kozieradzka-Kiszkurno, P. Świątek, Functional utrastructure of *Genlisea* (Lentibulariaceae) digestive hairs. *Ann. Bot.-London* **100**, 195–203 (2007).
7. Y. Heslop-Harrison, "Enzyme release in carnivorous plants" in *Lysosomes in Biology and Pathology*, J. Dingle, R. Dean, Eds. (North Holland, Amsterdam, The Netherlands, 1975), vol. 4, pp. 525–578.
8. B. Plachno *et al*., Fluorescence labelling of phosphatase activity in digestive glands of carnivorous plants. *Plant Biol.* **8**, 813–820 (2006).
9. H. Cao *et al*., Metatranscriptome analysis reveals host-microbiome interactions in traps of carnivorous *Genlisea* species. *Front. Microbiol.* **6**, 526 (2015).
10. B. Plachno, J. Faber, A. Jankun, Cuticular discontinuities in glandular hairs of *Genlisea* St.-Hil. in relation to their functions. *Acta Bot. Gallica* **152**, 125–130 (2005).
11. B. Juniper, R. Robins, D. Joel, *The Carnivorous Plants* (Academic Press, London, UK, 1989).
12. C. Carmesin *et al*., Structural gradients and anisotropic hydraulic conductivity in the enigmatic eel traps of carnivorous corkscrew plants (*Genlisea* spp.). *Am. J. Bot.* **108**, 2356–2370 (2021).
13. F. Caravieri *et al*., Bacterial community associated with traps of the carnivorous plants *Utricularia hydrocarpa* and *Genlisea filiformis*. *Aquat. Bot.* **116**, 8–12 (2014).
14. W. Barthlott, S. Porembski, E. Fischer, B. Gemmel, First protozoa-trapping plant found. *Nature* **392**, 447 (1998).
15. D. Darnowski, S. Fritz, Prey preference in *Genlisea* small crustaceans, not protozoa. *Carnivorous Plant Newsl.* **39**, 114–116 (2010).
16. N. P. Ni, B. Corominas-Murtra, C. Heisenberg, E. Hannezo, Rigidity percolation uncovers a structural basis for embryonic tissue phase transitions. *Cell* **184**, 1914 (2021).
17. A. Mashaghi, C. Dekker, Systems and synthetic biology approaches to cell division. *Syst. Synth. Biol.* **8**, 173 (2014).
18. R. Allen, B. Waclaw, Bacterial growth: A statistical physicist's guide. *Rep. Prog. Phys.* **82**, 016601 (2019).
19. S. Ramaswamy, The mechanics and statistics of active matter. *Annu. Rev. Condens. Matter Phys.* **1**, 323 (2010).
20. S. Ramaswamy, Active matter. *J. Stat. Mech: Theory Exp.* **70**, 054002 (2017).
21. C. Bechinger *et al*., Active particles in complex and crowded environments. *Rev. Mod. Phys.* **88**, 045006 (2016).
22. T. Vicsek, A. Zafeiris, Collective motion. *Phys. Rep.* **517**, 71 (2012).
23. M. C. Marchetti *et al*., Hydrodynamics of soft active matter. *Rev. Mod. Phys.* **85**, 1143 (2013).
24. J. Yan *et al*., Reconfiguring active particles by electrostatic imbalance. *Nat. Mater.* **15**, 1095 (2016).
25. S. van Kesteren, L. Alvarez, S. Arrese-Igor, L. I. A. Alegria, Self-propelling colloids with finite state dynamics. *Proc. Natl. Acad. Sci. U.S.A.* **120**, e2213481120 (2023).
26. C. Calero *et al*., Propulsion and energetics of a minimal magnetic microswimmer. *Soft Matter* **16**, 6673 (2020).
27. M. N. van der Linden, L. C. Alexander, D. G. A. L. Aarts, O. Dauchot, Interrupted motility induced phase separation in aligning active colloids. *Phys. Rev. Lett.* **123**, 098001 (2019).
28. H. R. Vutukuri, M. Lisicki, E. Lauga, J. Vermant, Light-switchable propulsion of active particles with reversible interactions. *Nat. Commun.* **11**, 2628 (2020).
29. J. Palacci *et al*., Light-activated self-propelled colloids. *Philos. Trans. R. Soc. A* **372**, 20130372 (2014).
30. M. E. Cates, J. Tailleur, When are active Brownian particles and run-and-tumble particles equivalent? Consequences for motility-induced phase separation. *Europhys. Lett.* **101**, 20010 (2013).
31. T. Qiu *et al*., Swimming by reciprocal motion at low Reynolds number. *Nat. Commun.* **5**, 5119 (2014).
32. H. C. Berg, D. A. Brown, Chemotaxis in *Escherichia coli* analysed by three-dimensional tracking. *Nature* **239**, 500 (1972).
33. K. Thornton, J. Butler, S. Davis, B. Baxter, L. Wilson, Haloarchaea swim slowly for optimal chemotactic efficiency in low nutrient environments. *Nat. Commun.* **11**, 4453 (2020).
34. L. Xie, T. Altindal, S. Chattopadhyay, X. L. Wu, Bacterial flagellum as a propeller and as a rudder for efficient chemotaxis. *Proc. Natl. Acad. Sci. U.S.A.* **108**, 2246–2251 (2011).
35. K. Son, J. Guasto, R. Stocker, Bacteria can exploit a flagellar buckling instability to change direction. *Nat. Phys.* **9**, 494–498 (2013).
36. J. Armitage, R. Schmitt, Bacterial chemotaxis: *Rhodobacter sphaeroides* and *Sinorhizobium meliloti*–Variations on a theme? *Microbiology* **143**, 3671–3682 (1997).
37. P. Galajda, J. Keymer, P. Chaikin, R. Austin, A wall of funnels concentrates swimming bacteria. *J. Bacteriol.* **189**, 8704–8707 (2007).
38. T. Zhou *et al*., AI-aided geometric design of anti-infection catheters. *Sci. Adv.* **10**, eadj1741 (2024).
39. V. Kantsler, J. Dunkel, M. Polin, R. Goldstein, Ciliary contact interactions dominate surface scattering of swimming eukaryotes. *Proc. Natl. Acad. Sci. U.S.A.* **110**, 1187–1192 (2013).
40. C. Reichhardt, C. J. O. Reichhardt, Crossover from intermittent to continuum dynamics for locally driven colloids. *Phys. Rev. Lett.* **96**, 028301 (2006).
41. R. Martinez, F. Alarcon, D. R. Rodriguez, J. L. Aragones, C. Valeriani, Collective behavior of Vicsek particles without and with obstacles. *Eur. Phys. J. E, Soft Matter* **41**, 91 (2018).
42. J. van Houten, E. Martel, T. Kasch, Fluorescence labelling of phosphatase activity in digestive glands of carnivorous plants. *J. Protozool.* **29**, 226–230 (1982).
43. W. Foissner, *Protozoa in Reference Module in Earth Systems and Environmental Sciences* (Elsevier, 2014).
44. X. Raynaud, N. Nunan, Spatial ecology of bacteria at the microscale in soil. *PLoS ONE* **9**, e87217 (2014).
45. D. Lundberg *et al*., Defining the core *Arabidopsis thaliana* root microbiome. *Nature* **488**, 86–90 (2012).
46. L. Turner, L. Ping, M. Neubauer, H. Berg, Visualizing flagella while tracking bacteria. *Biophys. J.* **111**, 630–639 (2016).
47. C. Reichhardt, C. J. Olson Reichhardt, Directional locking effects and dynamics for particles driven through a colloidal lattice. *Phys. Rev. E* **69**, 041405 (2004).

48. R. Martinez, F. Alarcon, J. L. Aragones, C. Valeriani, Trapping flocking particles with asymmetric obstacles. *Soft Matter* **16**, 4739 (2020).
49. S. Anand, X. Ma, S. Guo, S. Martiniani and X. Cheng, Transport and Energetics of Bacterial Rectification. arXiv [Preprint] (2024). https://arxiv.org/abs/2308.08421 (accessed 20 June 2024).
50. B. Płachno, K. Adamus, J. Faber, J. Kozłowski, Feeding behaviour of carnivorous *Genlisea* plants in the laboratory. *Acta Bot. Gallica* **152**, 159–164 (2005).
51. Y. Heslop-Harrison, "Unknown" in *Lysosomes in Biology and Pathology*, J. Dingle, R. Dean, Eds. (North Holland, Amsterdam, The Netherlands, 1975), vol. 4, pp. 525–578.
52. S. McPherson, *Glistening Carnivores–The Sticky-Leaved Insect-Eating Plants* (Redfern Natural History Productions, 2008).
53. J. Perrin, *Atoms* (D. Van Nostrand Company, New York, NY, 1916).
54. L. Wilson, R. Zhang, 3D localization of weak scatterers in digital holographic microscopy using Rayleigh–Sommerfeld back-propagation. *Opt. Express* **20**, 16735–16744 (2012).
55. L. G. Wilson *et al*., Differential dynamic microscopy of bacterial motility. *Phys. Rev. Lett.* **106**, 018101 (2011).